Inorganic Chemistry

Article

Cite This: Inorg. Chem. XXXX, XXX, XXX−XXX

pubs.acs.org/IC

Ligand Effect on the Single-Molecule Magnetism of Tetranuclear Co(II) Cubane

Xiong-Feng Ma,[†] Zhenxing Wang,[‡] Xue-Li Chen,[§] Mohamedally Kurmoo,*[,∥] and Ming-Hua Zeng*[,†,§]

[†]Key Laboratory for the Chemistry and Molecular Engineering of Medicinal Resources, School of Chemistry and Pharmaceutical Sciences, Guangxi Normal University, Guilin 541004, People's Republic of China

[‡]Wuhan National High Magnetic Field Center, Huazhong University of Science and Technology, Wuhan 430074, People's Republic of China

[§]Hubei Collaborative Innovation Center for Advanced Organic Chemical Materials, Ministry of Education Key Laboratory for the Synthesis and Application of Organic Functional Molecules, College of Chemistry and Chemical Engineering, Hubei University, Wuhan 430062, People's Republic of China

[∥]Institut de Chimie de Strasbourg, CNRS-UMR7177, Université de Strasbourg, 67070 Strasbourg, France

Supporting Information

ABSTRACT: A clear dependence on the ligand has been observed for the magnetic properties of a closely related series of Co(II) cubane structures, viz. $[Co_4(mbm \text{ or } bm)_4(ROH)_4Br_4]$ (**1-MeOH**, **1-EtOH**, **2-MeOH**, and **2-EtOH**, where **1** = $[Co_4(mbm)_4Br_4]$, **2** = $[Co_4(bm)_4Br_4]$, *bm* = (1*H*-benzo[*d*]imidazol-2-yl)methanolate. and *mbm* = 1-Me-*bm*.) The $[Co_4(OR)_4]$ cubane core consists of an octahedral Co^{II} center chelated by the alkoxide oxygen and imidazole nitrogen atoms from monoanionic *bm* or *mbm* and coordinated by methanol/alcohol and bromine. Interestingly, electrospray ionization mass spectrometry (ESI-MS) indicates that **1-MeOH** and **2-MeOH** are unstable in methanol and transformed to the butterfly $[Co_4L_6]^{2+}$ but that **1-EtOH** and **2-EtOH** are stable in ethanol. Their magnetic susceptibilities suggest ferromagnetic coupling between the nearest cobalt centers to give a theoretical $S = 4 \times 3/2$ ground state with considerable magneto-crystalline behavior. The packing and intermolecular interactions appear to influence the geometry of the cubes and thus the anisotropy of cobalt, which leads to different blocking temperatures (T_B). Consequently, the compounds with *mbm*, **1-MeOH** and **1-EtOH**, exhibit $T_B > 2$ K as shown by the relaxation of magnetization in zero applied dc field where the barriers U_{eff}/k_B are respectively 27 and 21 K and relaxation times are $\tau_0 = 1.3 \times 10^{-9}$ and 9.7×10^{-9} s. However, the compounds with *bm*, **2-MeOH** and **2-EtOH**, remain paramagnetic above 2 K and do not show nonlinear response of the ac susceptibilities. These findings reaffirm the subtle dependence of single-molecule magnetism on coordination geometry and intermolecular interaction.

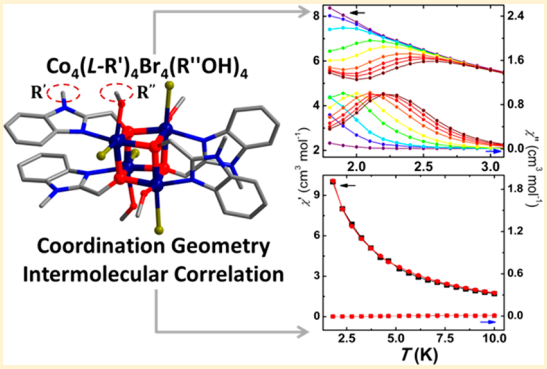

INTRODUCTION

The discovery of blocking of the magnetic moments within an individual molecular cluster, $[Mn_{12}O_{12}(CH_3COO)_{16}(H_2O)_4]$, brought about a new direction in the chemistry and physics of magnetic materials, which is now classed as single-molecule magnetism.[1−4] Its extension to single ions of several transition and lanthanide metals was reported 15 years later.[5−7] These advances were important deviations from previous works performed on nanoparticles,[8] allowing for direct evidence of quantum magnetism.[9,10] The beauty of this discovery lies in that every quantum level can be accounted for and every level of approximation in the hyperfine structures can be revealed by appropriate experimentations.[11,12] With the realization that the anisotropy of the ions forming the cluster defines very much the overall behavior of the magnetic properties, work has progressed from the mixed-valence $Mn^{III}_8Mn^{IV}_4$ to the single-valence clusters containing the more anisotropic first-row divalent transition metals (Fe, Co, and Ni), as they can form isostructural structures but with varying magnetic anisotropy.[13−16] Further extension using lanthanide ions, in particular dysprosium due to its high anisotropy, has also been carried out, and very high blocking temperatures have been reported.[17−21]

Numerous compounds of these divalent cobalt clusters have now been realized showing single-molecule magnetism.[22−32] However, a large number do not display these properties in the temperature operable by the commercial SQUID magnetometers used for the measurements.[33−35] Following certain guidelines developed over the years, chemists have been

Received: October 1, 2017

DOI: 10.1021/acs.inorgchem.7b02530
Inorg. Chem. XXXX, XXX, XXX−XXX

designing organic ligands using very different approaches to generate materials that can be operated as magnets at higher temperatures: i.e., those with high blocking temperatures. The principal parameters aimed at are the magnitude and sign of the magneto-crystalline anisotropy.[22,36]

Numerous works along these lines have focused on the use of benzimidazole derivatives with transition metals of the first row.[24−28] A literature search on this family of ligands reveals that a range of complexes form monomers,[37] dimers,[38] cubanes,[25,39−41] disks,[38,40] and chains.[42] A number of materials have been reported, with some displaying SMM at a moderate blocking temperature of 4 K.[22−32] The high-spin states in the cubane compounds were warranted by the ferromagnetic exchange between edge-sharing octahedra of divalent Fe (d^6),[13,39] Co (d^7),[15,22,29,34,38,40] and Ni (d^8).[16,25] Several factors affecting the magnetic properties of the cluster were investigated to explore ways to improve the SMM properties. For a cubane-based, triangular Co_{12} SMM, the effects of metal ions (Co^{II} and Ni^{II}) and counteranions on the structure and magnetic behavior were investigated.[24,25] It is also found that interchanging the inner bridges (OH^-, OCH_3^-, and N_3^-) can significantly change their stability in solution and their magnetic properties without affecting the overall topology of the Co_7 brucite disk clusters.[27] The frustrated magnetic properties of a multifaceted cage cluster with halide templates of Cl^- and Br^- were found to be related to the association of host−guest interactions.[28] The effect of substituted groups extending in the salicylaldehyde Schiff base ligands on both Co_7 disks and Co_4 cubes was also identified.[33,34] Very recently, we have also found an interesting solid−gas reaction of a nonporous Fe_4 cube compound and estimated the effect of postsynthetic oxidation on the magnetism.[39] As a result, the magnetic ground state, blocking temperature, energy barrier, and relaxation time of the above compound were modified to a certain extent. Even so, systematically changing both the substituted groups of the main ligand and the terminal solvents or ions of the cube cluster to build a model system is difficult. There is also little understanding about the dependence of cube SMMs on coordination geometry and intermolecular interaction.

Hence, we report results pertaining to a series of related cobalt(II) compounds where we have varied two parameters: the substituent of the ligand (H versus CH_3) and the coordinating solvent (methanol versus ethanol) (Scheme 1). Surprisingly, the two compounds containing the methyl-substituted ligand exhibit SMM but those without do not.

Scheme 1. Molecular Structures of the Ligands and an Example of a [Co_4O_4] Cube Structure Highlighting the Different Chemical Modifications

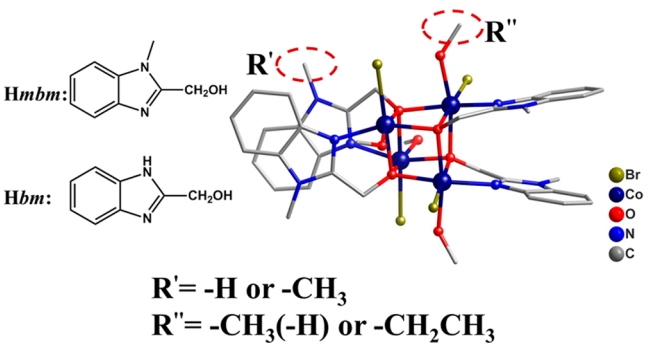

The search for this difference is examined by detailed crystallography and exploration of the magnetic properties.

RESULTS AND DISCUSSION

Crystal Structure. The compounds have one common structural motif consisting of a Co_4O_4 core in the form of a cube with the Co and O occupying opposite corners (Figure 1).

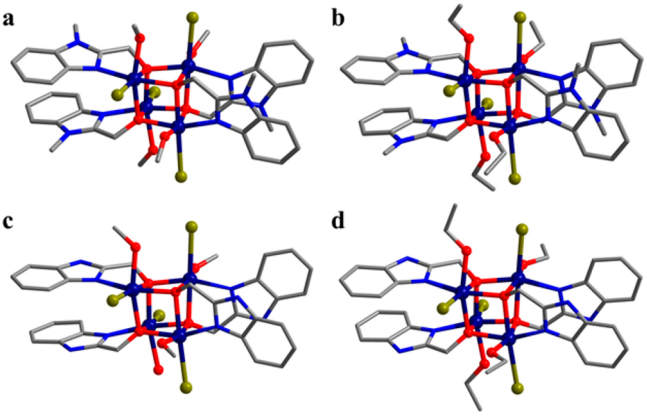

Figure 1. Crystal structures of the four cubanes **1-MeOH** (a), **1-EtOH** (b), **2-MeOH** (c), and **2-EtOH** (d).

In other words, one can consider it as the interpenetration of two tetrahedral sublattices. The cube is distorted and thus allows for a range of crystal symmetries, as can be seen by the different space groups of the four examples of this work (Table 1). Each metal adopts a distorted-octahedral geometry consisting of chelating organic ligands (*mbm* and *bm*) where the nitrogen is singly bonded but the alkoxide oxygen atom acts as a triple bridge at the corner of the cube (Table S1 in the Supporting Information). The remaining two sites are then taken by the bromine and oxygen of the solvent (ethanol or methanol). For highly symmetric structures, *P*4 or *I*4, the metal centers are equivalent, but they can be very different in the low-symmetry triclinic systems, where the solvents and Br sites can also be different.

The Co_4O_4 core is a fairly stable geometry with Co−O and Co−N distances lying within observed ranges of coordination compounds and the angles vary in a wider range (Table 2). The Co···Co distances which are relevant to the magnetism are normal to those bridged by two oxygen atoms. However, they can vary in the range 97−100°, which can favor either ferromagnetic or antiferromagnetic coupling depending on which side of the Goodenough−Kanamori crossover angle each pair sits.[43,44] Thus, there are subtle changes in the magnetism that are dependent on these angles.

In all cases the chelating organic ligands are paired face to face on opposite side of the cube. This leaves the solvent and the halogen atoms to lie in a plane perpendicular to that of the organic ligands. This choice of geometry favors an efficient packing and allows for supramolecular interaction between molecules (Figure S1 in the Supporting Information).

The coordination geometry of the cobalt centers defines the magnitude and signs of the crystal field parameters and therefore the magnetic properties of the individual magnetic centers.[22,45] In addition, the exchange interaction between all nearest neighbors leads to a particular temperature dependence of the magnetic susceptibility characteristic of the cluster. Since the parameters spin−orbit coupling, single-ion anisotropy

DOI: 10.1021/acs.inorgchem.7b02530
Inorg. Chem. XXXX, XXX, XXX−XXX

Table 1. Crystal and Structure Refinement Data for 1-MeOH, 2-MeOH, 1-EtOH, and 2-EtOH

	1-MeOH	2-MeOH	1-EtOH	2-EtOH
formula	$C_{40}H_{52}Br_4Co_4N_8O_8$	$C_{37}H_{50}Br_4Co_4N_8O_{10}$	$C_{44}H_{60}Br_4Co_4N_8O_{10}$	$C_{40}H_{52}Br_4Co_4N_8O_8$
formula wt	1328.25	1322.21	1416.36	1328.26
temp (K)	296(2)	296(2)	296(2)	296(2)
cryst syst	orthorhombic	triclinic	tetragonal	tetragonal
space group	$P2_12_12_1$	$P\bar{1}$	$P\bar{4}2_1c$	$I4_1/a$
a (Å)	11.1744(11)	11.133(17)	13.252(5)	17.063(10)
b (Å)	11.1750(11)	14.03(2)	13.252(5)	17.063(10)
c (Å)	39.104(4)	16.51(3)	17.509(12)	17.384(10)
α (deg)	90	88.424(18)	90	90
β (deg)	90	70.758(17)	90	90
γ (deg)	90	86.457(19)	90	90
V (Å^3)	4883.1(8)	2431(7)	3075(3)	5061(5)
Z	4	2	2	4
D_c (g cm^{-3})	1.807	1.807	1.530	1.743
F(000)	2640	1312	1416	2640
μ (mm^{-1})	4.665	4.688	3.712	4.501
no. of rflns collected	39906	22501	31713	28551
no. of unique rflns	11125	10467	3018	2552
R_{int}	0.0338	0.1164	0.0669	0.0436
R1,[a] wR2[b] ($I > 2\sigma(I)$)	0.0366, 0.0869	0.0709, 0.1755	0.0378, 0.0960	0.0284, 0.0672
R1, wR2 (all data)	0.0368, 0.0870	0.2039, 0.2458	0.0581, 0.1054	0.0410, 0.0751
GOF	1.184	0.954	1.065	1.101

[a] $R1 = \sum||F_o| - |F_c||/\sum|F_o|$. [b] $wR2 = [\sum w(F_o^2 - F_c^2)_2/\sum w(F_o^2)_2]^{1/2}$.

Table 2. Ranges of Bond Lengths and Angles for 1-MeOH, 2-MeOH, 1-EtOH, and 2-EtOH

	1-MeOH	2-MeOH	1-EtOH	2-EtOH
Co−Br (Å)	2.528−2.543	2.523−2.632	2.584	2.565
Co−N (Å)	2.055−2.106	2.051−2.122	2.100	2.089
Co−O (Å)	2.047−2.156	2.056−2.166	2.082−2.116	2.076−2.157
Co−O(solvent) (Å)	2.120−2.174	2.130−2.202	2.131	2.180
O−Co−O (deg)	79.2−82.2	79.3−82.0	78.9−81.8	80.3−80.7
Co···Co (Å)	3.153−3.283	3.152−3.256	3.176−3.297	3.209−3.260
O−Co−N (deg)	76.8−101.5	77.8−103.1	78.4−99.3	78.3−101.9
Co−O−Co (deg)	96.9−100.1	96.5−100.3	96.9−100.8	98.57−99.08

terms (D and E), and exchange interaction collectively contribute to variation in the magnetic susceptibility with temperature and the isothermal magnetization as a function of field, their magnitudes and signs are important in the final ground state of the clusters.[35] Thus, a comparison of the bond lengths and angles within and between the clusters are given in Table 2.

Several supramolecular interactions, including C−H···Br, C(Me)-H···O, C(Me)−H···π, and π···π, are present within the structures.[26,34] The bidentate organic ligands are paired and located on the opposite face of the cube, and the pairs are pseudo-orthogonal. The imidazole rings of each *mbm/bm* exhibit strong π···π interactions where the center to center distances fall in the range 3.42−3.50 Å. The second important interaction is that the terminally coordinated Br is connected diagonally through an O−H···Br H bond to the coordinated alcohol.

However, because of the different substituent groups of the bidentate ligands and coordinated solvent molecules and, most importantly, the different crystal symmetries, the supramolecular interactions are different in the structures. Whether and how these differences play important roles in influencing the magnetic properties are interesting questions. For **1-MeOH**, each $[Co_4O_4]$ cube neighbors four others via C(Me)−H···Br interactions and eight others via C(Me)−H···π interactions (Figure 2); thus, it can be considered as forming a 12-connected *fcu* net (Figure S2a in the Supporting Information) with distances of 11.17−12.91 Å between the centers of the $[Co_4O_4]$ cubes. In contrast, **1-EtOH** forms an 8-connected *bcu* net (Figure S2b) via C−H···Br H bonds between Br and benzimidazole (Figure S1a in the Supporting

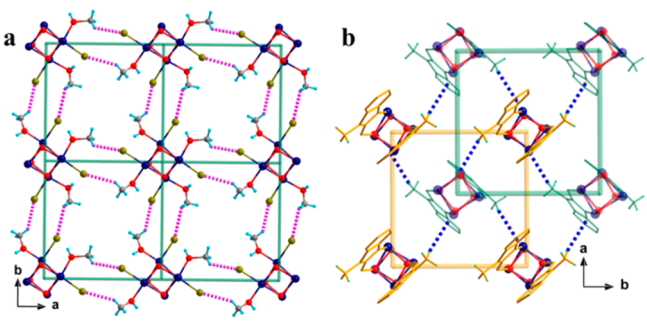

Figure 2. Structure of **1-MeOH** showing the supramolecular interactions: (a) C(Me)−H···Br H bond (purple dotted line) connecting clusters within a (4,4) layer; (b) C(Me)−H···π bond (blue dotted line) between layers.

DOI: 10.1021/acs.inorgchem.7b02530
Inorg. Chem. XXXX, XXX, XXX−XXX

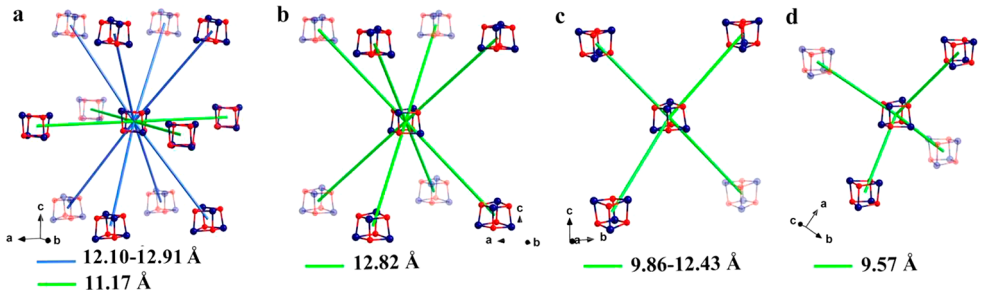

Figure 3. Connecting modes of the clusters through C(Me)−H···π interactions and/or hydrogen bonds in (a) **1-MeOH**, (b) **1-EtOH**, (c) **2-MeOH**, and (d) **2-EtOH**.

Information). The shortest distance between the centers of the $[Co_4O_4]$ cubes is 12.82 Å (Figure 2b). Among the compounds **1-EtOH** is the least well packed, as judged by the low density of 1.53 g/cm^3 in comparison to 1.74−1.80 g/cm^3 for the others. This ineffective packing allows space for water molecules within the lattice, determined to be two molecules that are disordered (unable to refine with anisotropic thermal parameters) from X-ray diffraction but three molecules by thermogravimetric analysis (Figure S3 and Table S2 in the Supporting Information).

For the two compounds containing *bm* ligands, **2-MeOH** and **2-EtOH** (Figure 3c,d), the $[Co_4O_4]$ cubes are marginally smaller than those with *mbm*, **1-MeOH** and **1-EtOH** (Figure 3a,b), resulting in nearest-neighbor intermolecular distances of 9.86 and 9.57 Å, respectively. Even though they crystallize in very contrasting space groups, $P\bar{1}$ and $I4_1/a$, each cluster of **2-MeOH** and **2-EtOH** is connected to four neighbors through N/C−H···Br H bonds (Figure S1b,c in the Supporting Information) resulting in the 4-connected *diamond* net (Figure S2c,d in the Supporting Information).

Electrospray Ionization Mass Spectrometry. The positive ion ESI-MS spectra of the compounds (Figure 4 and Figures S4−S7 in the Supporting Information) display contrasting behaviors which depend on the coordinating alcohol. For example, the highest intensity peaks of the methanol-containing compounds do not correspond to their integral molecular units; instead, they correspond to the new fragments $[Co_4L_6]^{2+}$. This observation suggests that Co_4L_4 possibly transformed in methanol for both *mbm* and *bm*. For **1-MeOH** the peak at *m*/*z* 601.08 corresponds to $[Co_4(mbm)_6]^{2+}$ (calculated *m*/*z* 601.08). The low-intensity peaks at *m*/*z* 1070.87 and 1118.76 belong to the species $[Co_4(mbm)_4Br_2(CH_3O)]^+$ (1070.87) and $[Co_4(mbm)_4Br_3]^+$ (1118.77), suggesting that some Co_4L_4 remains, which is a phenomenon of CH_3O^- substituting for Br^-. It can be seen from Table S3 in the Supporting Information that **1-MeOH** undergoes not only cleavage under mass spectrometry conditions to low-nuclearity fragments such as Co_1, Co_2, and Co_3 but also oligomerization to Co_5, Co_6, and Co_7. It is surprising that the cluster $[Co_7(mbm)_{12}]^{2+}$ has been developed, which corresponds to the established brucite disk compound.[40] For **2-MeOH**, the peak at *m*/*z* 559.03 corresponds to $[Co_4(bm)_6]^{2+}$ (559.04). Those at *m*/*z* 1130.83 and 1198.97 correspond to $[KCo_4(bm)_4Br_2(OH)_2(H_2O)]^+$ (1130.83) and $[K_2Co_4(bm)_4Br(CH_3O)_4(H_2O)_2]^+$ (1198.96). It was observed from the data that Br^- in the framework of the structure may easily be separated under mass spectrometry due to the large ionic radius in the methanol system (Figure 4 and Table S3). The fragments observed for the negative ions are given in Table S4 and shown in Figures S8−S12 in the Supporting Information.

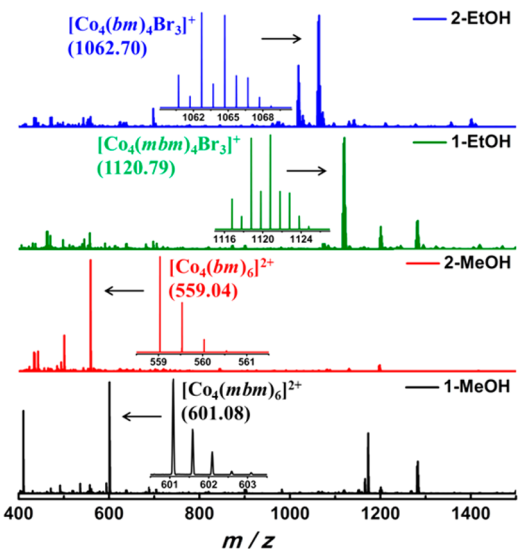

Figure 4. ESI-MS spectra of the solutions of dissolved crystals of **1-MeOH**, **2-MeOH**, **1-EtOH**, and **2-EtOH**. The insets give the expanded region of the highest intensity peaks.

For the ethanol-containing compounds the highest intensity peak corresponds to $[Co_4L_4Br_3]^+$, which contains the core clusters for both ligands *mbm* and *bm*. The peak at *m*/*z* 1120.79 is that of $[Co_4(mbm)_4Br_3]^+$ (1120.79), which also contains the Co_4L_4 core structure for **1-EtOH**. The situation is similar for the peak at *m*/*z* 1062.70 of **2-EtOH**, which is from $[Co_4(bm)_4Br_3]^+$ (1062.71) (Figure 4 and Table S3 in the Supporting Information). The stability in solution can be given in the following orders: **1-EtOH** > **1-MeOH** and **2-EtOH** > **2-MeOH**.

Magnetic Properties. The magnetic susceptibilities of polycrystalline samples of **1-MeOH**, **2-MeOH**, **1-EtOH**, and **2-EtOH** were measured on cooling from 300 to 1.8 K in an applied field of 100 or 1000 Oe (Figure 5). The values of $\chi_m T$ at 300 K fall in the range of 12.6−14.1 cm^3 K mol^{-1}, indicating an orbital contribution for octahedral Co(II). Upon cooling, $\chi_m T$ increases marginally up to ca. 100 K before going through shallow minima around 50 K. A peak is finally observed below 15 K. Analyses of the χ_m^{-1} vs T data above 150 K using the Curie−Weiss law give estimated Curie constants in the range of 12.25−13.97 cm^3 K mol^{-1} and Weiss constants (Θ) of +3.2 to +8.5 K (Figure S13 in the Supporting Information). The Curie constants are normal for octahedral Co(II), and the positive

DOI: 10.1021/acs.inorgchem.7b02530
Inorg. Chem. XXXX, XXX, XXX−XXX

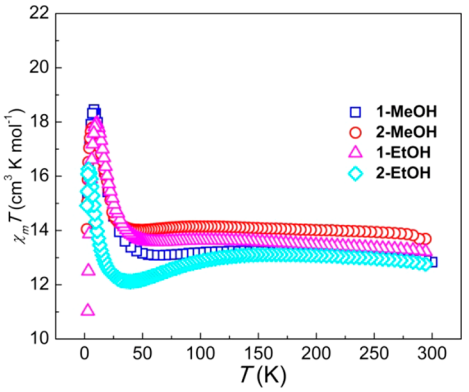

Figure 5. Temperature dependence of $\chi_m T$ for **1-MeOH**, **2-MeOH**, **1-EtOH**, and **2-EtOH**.

Weiss constants (Table 3) indicate intracluster ferromagnetic coupling.[46]

Table 3. $\chi_m T$ Values and Curie and Weiss Constants for 1-MeOH, 2-MeOH, 1-EtOH, and 2-EtOH

compound	$\chi_m T$(300 K) (cm^3 K mol^{-1})	$\chi_m T$(max) (cm^3 K mol^{-1})	C (cm^3 K mol^{-1})	Θ (K)
1-MeOH	12.59	18.02	12.25	+8.48
2-MeOH	14.06	17.87	13.97	+3.18
1-EtOH	13.39	17.96	13.18	+6.11
2-EtOH	12.95	16.27	12.89	+4.38

The temperature dependence of the moment (as represented by $\chi_m T$) is rather complex but has been seen in several clusters containing Co(II) in octahedral geometry. The high temperature is dominated by the nearest-neighbor ferromagnetic interaction giving an increase on lowering of the temperature. The appearance of the minimum is associated with the effect of spin−orbit coupling for each Co(II) center as a consequence of the depopulation of the excited state Kramers doublets. The final peak at lower temperature is caused by two effects: one is the single-ion anisotropy, and the other is saturation of the magnetization. As these parameters are related to one another, extracting them from susceptibility data is an enormous task. Several attempts to fit the data have so far failed to give reasonable and acceptable parameters due to their interrelations and failure to give a global minimum in the multidimensional space.[47]

The isothermal magnetization of each compound was measured at 2 K as a function of applied magnetic field up to 7 T following cooling in zero field (Figure S14 in the Supporting Information). In each case the magnetization shows a rapid increase below 10 kOe field, confirming the ferromagnetic nature of the exchange interaction, followed by a slow increase to high fields. The values reach 8.26 (**1-MeOH**), 9.49 (**2-MeOH**), 7.49 (**1-EtOH**) and 10.22 $N\beta$ (**2-EtOH**) at 7 T. Interestingly the *bm*-containing compounds have slightly lower saturation magnetization in comparison to those with *mbm*. The values are close to those expected for four Co(II) atoms of 9.6 $N\beta$ assuming 2.4 $N\beta$ per Co(II).[46] Assuming that only the ±1/2 Kramers doublet is populated at 2 K, the effective spin will be 1/2 and the total spin ground state for the cluster will be S_T = 2. Therefore, from the saturation magnetization values that are equal to gS_T, we estimate the g values as 4.13, 4.75, 3.75, and 5.11, respectively.

The ac susceptibilities were studied through three sets of measurements: (a) as a function of temperature for a range of frequencies spanning 1−997 Hz, (b) as a function of frequency using an oscillating field of 2.5 Oe in 0 or 750 Oe bias dc field, and (c) as a function of field at 2 K. Under a 0 dc field, only **1-MeOH** and **1-EtOH** exhibit nonlinear magnetization: i.e., nonzero out-of-phase susceptibility (χ''). The nonlinearity appears below 3 K for all frequencies in the range 1−1000 Hz (Figure 6). While χ'' peaks above 2 K for **1-MeOH** (Figure 6a), it does not for **1-EtOH** (Figure 6c). This suggests a difference in blocking temperatures or relaxation times. There is a continuous trend of the ac susceptibilities toward high temperature with increasing frequency. For **1-MeOH** and **1-EtOH** the relation $\Phi = (\Delta T_p/T_p)/(\Delta \log \nu)$ is obeyed, giving Φ = 0.26, which corresponds to that of a superparamagnet. However, in a bias dc field of 750 Oe **1-MeOH** and **1-EtOH** behave in an almost identical way (Figure S15 in the Supporting Information), suggesting a weak change in the energy levels. Whether this is due to the anisotropy lining up the cluster internal magnetic field with the external field or removal of the degeneracy of the α and β spin states remains to be determined.

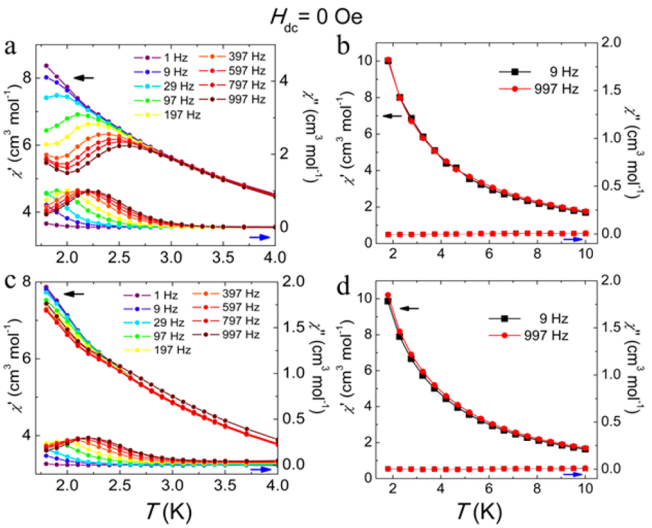

Figure 6. Temperature dependence of the in-phase (χ') and out-of-phase (χ'') ac susceptibilities for different frequencies in 0 dc field for (a) **1-MeOH**, (b) **2-MeOH**, (c) **1-EtOH**, and (d) **2-EtOH**.

The Cole−Cole plots (Figure 7 and Figure S16 in the Supporting Information) follow a single-relaxation Debye model. The fitting parameters τ (relaxation time) and α (α determines the width of the distribution of relaxation times) are given in Tables S5 and S6. The parameter α for **1-MeOH** and **1-EtOH** falls in the range of 0.1−0.35, which envelops those observed for Co^{II}-based SMMs and suggests a narrow to moderate distribution of magnetic relaxation. It is noted that the magnetic relaxation times for **1-EtOH** in 750 Oe external dc field are marginally longer than those in zero dc field. In contrast, no slowing of the magnetic relaxation process is observed for **1-MeOH**, indicating limited but not negligible quantum tunneling (Figure S17 in the Supporting Information).

The temperature-dependent relaxation times were analyzed assuming a thermally activated process following the Arrhenius law ($\tau = \tau_0 \exp(U_{eff}/k_B T)$). The energy barriers and

DOI: 10.1021/acs.inorgchem.7b02530
Inorg. Chem. XXXX, XXX, XXX−XXX

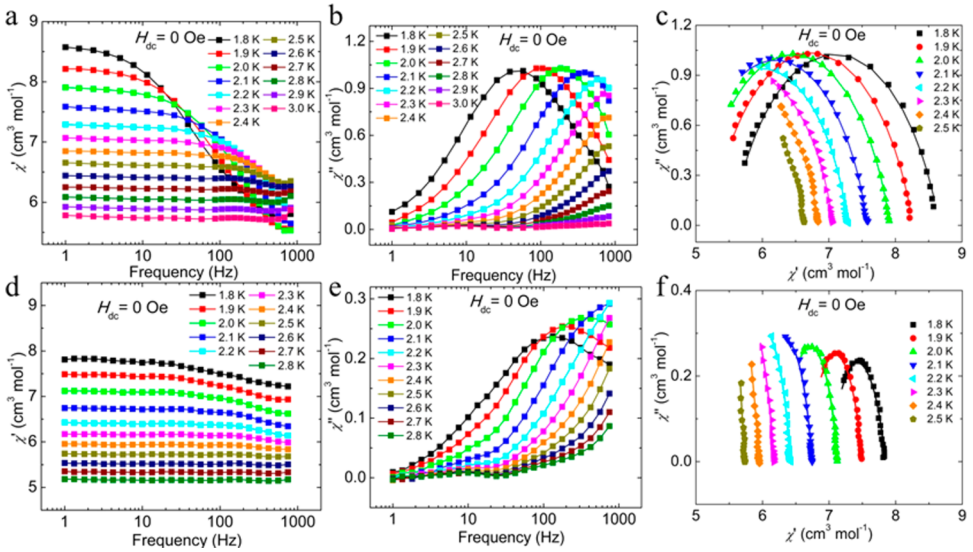

Figure 7. Variable-frequency ac susceptibilities (H_{dc} = 0 Oe) at different temperatures for (a, b) **1-MeOH**, and (d, e) **1-EtOH** and Cole−Cole plots from ac susceptibilities (H_{dc} = 0 Oe) for (c) **1-MeOH** and (f) **1-EtOH**.

extrapolated relaxation times were U_{eff} = 27 K and $\tau_0 = 1.3 \times 10^{-9}$ s for **1-MeOH** and U_{eff} = 21 K and $\tau_0 = 9.7 \times 10^{-9}$ s for **1-EtOH** under 0 dc field (Figure 8a). Under 750 Oe dc field, the values are U_{eff} = 27 K and $\tau_0 = 1.3 \times 10^{-9}$ s for **1-MeOH** and U_{eff} = 26 K and $\tau_0 = 5.6 \times 10^{-9}$ s for **1-EtOH** (Figure 8b). The parameters of the present compounds are compared to those for several well-characterized cubane compounds (Table 4).

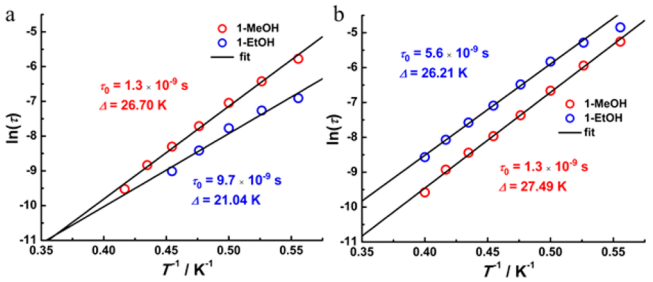

Figure 8. Arrhenius plots generated from the temperature-dependent relaxation times extracted from the ac susceptibility Cole−Cole fits for **1-MeOH** and **1-EtOH** in (a) H_{dc} = 0 Oe and (b) H_{dc} = 750 Oe. Symbols give extracted times, and lines give least-squares fits.

In contrast, **2-MeOH** (Figure 6b) and **2-EtOH** (Figure 6d) display no out-of-phase component of the ac susceptibilities in 0 dc field for frequencies of 1 and 997 Hz down to 2 K. The real component of the ac susceptibilities as a function of dc field was found to maximize at 5000 Oe. Using 5000 Oe as the bias field, the real part of the ac susceptibilities shows a maximum at 4.2 and 3.7 K, respectively, but no imaginary component was observed (Figure S15 in the Supporting Information). This indicates that there is no blocking of the moments above 2 K.

CONCLUSION

When the size of the chelating organic ligand was varied from (1*H*-benzo[*d*]imidazol-2-yl)methanolate to its methyl-substituted *N*-methyl-(1*H*-benzo[*d*]imidazol-2-yl)methanolate in the Co(II) cubane, a major difference in magnetic properties was

Table 4. Behaviors as well as the Gap Energies and Relaxation Times for the Compounds Containing Co_4O_4 Units

cluster[a]	ΔE (K)	τ_0 (10^{-9} s)	Co···Co (Å)	Co−O−Co (deg)
$[Co_4(hmp)_4(MeOH)_4Cl_4]$[14]	24	34	3.18−3.26	96.84−100.74
$[Co_4L_4]$[15]	64.4	3.8	3.12−3.26	93.35−101.63
$[Co_{12}(bm)_{12}(NO_3)(O_2CMe)_6(EtOH)_6](NO_3)_5$[24]	15	190	3.03−3.24	95.66−102.07
$[Co_{12}(bm)_{12}(NO_3)(O_2CMe)_6(EtOH)_6](ClO_4)_5$[25]	24	310	3.03−3.24	95.66−102.07
$[Co_7(bhqe)_3(OH)_2(H_2O)_6]\cdot 2C_2H_5OH\cdot H_2O$[26]	21(4)	270	3.05−3.18	91.50−99.86
$[(NMe_4)_3Na\{Co_4(cit)_4[Co(H_2O)_5]_2\}]\cdot 11H_2O$[48]	26	8.2	3.13−3.22	96.46−100.33
$[(NMe_4)_4\{Co_4(cit)_4[Co(H_2O)_5]_2\}]\cdot 6H_2O$[48]	32	2.1		96.46−100.33
$[C(NH_2)_3]_8[Co_4(cit)_4]\cdot 4H_2O$[49]	21	800		97.18−99.24
$[C(NH_2)_3]_8[Co_4(cit)_4]\cdot 8H_2O$[50]	13.1	840	3.17−3.22	97.18−99.24
$[Co_8(C_4O_7)_4(H_2O)_{12}]\cdot 24H_2O$[50]	20.5	100	3.21	100.40
$[Co_4(hmb)_4(\mu_3\text{-}OMe)_4(MeOH)_4]$[51]	60.8	25	3.11−3.16	95.21−98.30
$[Co_7(OH)_8(tta)_6(ROH)_6]\cdot ROH$ (R = isopropyl)[52]	22	8.2	3.10−3.13	95.89−98.41
$[Co_7(OH)_8(tta)_6(ROH)_6]\cdot ROH$ (R = *n*-butyl)[52]	21	3.4	3.09−3.15	95.35−100.65
$[Co_4(mbm)_4Br_4(CH_3OH)_4]$ (this work)	26.7	1.3	3.15−3.28	96.90−100.24
$[Co_4(mbm)_4Br_4(CH_3CH_2OH)_4]$ (this work)	21.0	9.7	3.18−3.30	96.92−100.55

[a]Abbreviations: hmp = hydroxymethylpyridine; H_2L = 2-(1-(2-hydroxyethyl)-1*H*-pyrazol-3-yl)phenol; H_4bhqe = 1,2-bis(8-hydroxyquinolin-2-yl)ethane-1,2-diol; cit = citrate; Hhmb = 2-hydroxy-3-methoxybenzaldehyde; tta = 4,4,4-trifluoro-1-thienoyl-2,4-butanedionate.

DOI: 10.1021/acs.inorgchem.7b02530
Inorg. Chem. XXXX, XXX, XXX−XXX

observed, in contrast to the minimal effect by replacing the coordinating methanol by ethanol. In the absence of any major deviations in the coordination parameters (bond lengths and angles) and relatively similar intermolecular interactions, we are left to believe that the small differences in electronic effect may be enough to tune the magneto-crystalline parameters to vary the blocking temperature. However, for the present set of compounds the numbers of neighbors are different—those with 12 or 8 have higher T_B values in comparison to those with 4. Further work will be needed to get a complete picture of these magnetic property differences. This is the first time that a systematic and comprehensive study of the magnetic properties has been carried out for a series of cobalt clusters to show such small, subtle dependence.

EXPERIMENTAL SECTION

Materials and Measurements. All reagents were obtained from commercial sources and used without further purification. Elemental analyses for C, H, and N were performed on a Vario Micro Cube. Thermogravimetric analyses (TGA) were performed under a flow of nitrogen at a heating rate of 10 °C/min using a NETZSCH TG 209 F3 instrument. Infrared spectra were recorded by transmission through KBr pellets containing ca. 0.5% of the compounds using a PE Spectrum FT-IR spectrometer (400−4000 cm^{-1}). Magnetization measurements were performed for polycrystalline samples between 2 and 300 K and at ±70 kOe using a Quantum Design VSM-SQUID magnetometer. ac susceptibilities were measured as a function of temperature and frequency (1−1000 Hz) in an oscillating field of 2.5 Oe using the same magnetometer.

Synthesis. A mixture of $CoBr_2$ (1.0 mmol, 218 mg), H*mbm* or H*bm*[53] (2.0 mmol, 324 or 296 mg), triethylamine (0.1 mL), and methanol or ethanol (8 mL) was stirred and sealed in a 15 mL Teflon-lined stainless steel autoclave and heated to 140 °C for 2 days. It was then cooled to room temperature over 1 day. Wine red octahedral shaped crystals of **1-MeOH**, **2-MeOH**, **1-EtOH**, and **2-EtOH** were obtained.

1-MeOH. $[Co_4(mbm)_4Br_4(CH_3OH)_4]$: yield 210 mg, 63.4% (based on $CoBr_2$). Anal. Calcd: C, 36.17; H, 3.95; N, 8.44. Found: C, 35.97; H, 3.51; N, 8.18. Selected IR bands (KBr, cm^{-1}), 3261 (vs), 2944 (s), 1491 (m), 1064 (s), 751 (m).

2-MeOH. $[Co_4(bm)_4Br_4(CH_3OH)_3(H_2O)]\cdot 2CH_3OH$: yield 200 mg, 63.8% (based on $CoBr_2$). Anal. Calcd: C, 33.61; H, 3.81; N, 8.47. Found: C, 33.27; H, 3.19; N, 8.58. Selected IR bands (KBr, cm^{-1}), 3241 (vs), 2907 (s), 1452 (m), 1064 (s), 752 (m).

1-EtOH. $[Co_4(mbm)_4Br_4(CH_3CH_2OH)_4]\cdot 3H_2O$: yield 230 mg, 66.8% (based on $CoBr_2$). Anal. Calcd: C, 36.74; H, 4.62; N, 7.79. Found: C, 36.46; H, 4.34; N, 7.90. Selected IR bands (KBr, cm^{-1}), 3459 (vs), 2831 (s), 1488 (m), 1065 (s), 746 (m).

2-EtOH. $[Co_4(bm)_4Br_4(CH_3CH_2OH)_4]$: yield 180 mg, 54.2% (based on $CoBr_2$). Anal. Calcd: C, 36.17; H, 3.95; N, 8.44. Found: C, 36.51; H, 3.77; N, 8.42. Selected IR bands (KBr, cm^{-1}), 3195 (vs), 2971 (s), 1452 (m), 1063 (s), 739 (m).

Crystallographic Studies. Single-crystal X-ray diffraction data for **1-MeOH**, **2-MeOH**, **1-EtOH**, and **2-EtOH** were collected on Bruker Smart Apex CCD and Agilent Supernova CCD diffractometers. Both employed graphite-monochromated Mo Kα radiation. The structures were solved by direct methods and refined by least-squares minimization. The $F_o - F_c$ maps identified all the hydrogen atoms with electron densities higher than 2σ level. **1-MeOH** had intrinsically poor crystallinity due to twinning, and diffraction data from several crystals did not lead to high-quality refinements. We therefore report the best result as judged from the reliability factors for a twinned crystal. A similar cubiclike structure with a different coordinated halogen ion has been reported for **1-EtOH**. The CCDC reference numbers are 1568807 (**1-MeOH**), 1568805 (**2-MeOH**), 1568804 (**1-EtOH**), and 1568806 (**2-EtOH**).

Mass Spectrometry Measurements. ESI-MS measurements were conducted at a capillary temperature of 275 °C. Aliquots of the solution were injected into the device at 0.3 mL/h. The mass spectrometer used for the measurements was a ThermoExactive instrument, and the data were collected in positive and negative ion mode. The spectrometer was previously calibrated with the standard tune mix to give a precision of ca. 2 ppm in the region of m/z 400−2000. The capillary voltage was 50 V, the tube lens voltage was 150 V, and the skimmer voltage was 25 V. The in-source energy was set to a range of 0 eV with a gas flow rate at 10% of the maximum.

ASSOCIATED CONTENT

Supporting Information

The Supporting Information is available free of charge on the ACS Publications website at DOI: 10.1021/acs.inorgchem.7b02530.

Bond parameters, crystal data, TGA data, ESI-MS spectra and assignments, magnetic susceptibility data, and isothermal magnetization data at 2 K (PDF)

Accession Codes

CCDC 1568804−1568807 contain the supplementary crystallographic data for this paper. These data can be obtained free of charge via www.ccdc.cam.ac.uk/data_request/cif, or by emailing data_request@ccdc.cam.ac.uk, or by contacting The Cambridge Crystallographic Data Centre, 12 Union Road, Cambridge CB2 1EZ, UK; fax: +44 1223 336033.

AUTHOR INFORMATION

Corresponding Authors

*E-mail for M.K.: kurmoo@unistra.fr.

*E-mail for M.-H.Z.: zmh@mailbox.gxnu.edu.cn.

ORCID

Zhenxing Wang: 0000-0003-2199-4684

Mohamedally Kurmoo: 0000-0002-5205-8410

Ming-Hua Zeng: 0000-0002-7227-7688

Author Contributions

The experiments were performed by Xiong-Feng Ma, Zhenxing Wang, and Xue-Li Chen under the direction of Ming-Hua Zeng and Mohamedally Kurmoo.

Notes

The authors declare no competing financial interest.

ACKNOWLEDGMENTS

This work was supported by the National Science Foundation for Distinguished Young Scholars of China (No. 21525101), the NSF of China and Guangxi Province (No. 91422302, No. 21371037, 2014GXNSFFA118003, 2017GXNSFDA198040), the BAGUI scholar program (2014A001), the Project of Talents Highland of Guangxi Province, and the Opening Project of Wuhan National High Magnetic Field Center in the Huazhong University of Science and Technology (Grant No. 2015KF05). M.K. is supported by the CNRS-France.

REFERENCES

(1) Sessoli, R.; Gatteschi, D.; Caneschi, A.; Novak, M. A. Magnetic bistability in a metal-ion cluster. *Nature* **1993**, *365*, 141−143.

(2) Gatteschi, D.; Sessoli, R.; Villain, J. *Molecular Nanomagnets*; Oxford University Press: Oxford, U.K., 2006.

(3) Winpenny, R. E. P. Single-Molecule Magnets and Related Phenomena. *Struct. Bonding (Berlin)* **2006**, *122*, 1−250.

(4) Zhang, P.; Guo, Y.-N.; Tang, J. K. Recent advances in dysprosium-based single molecule magnets: Structural overview and synthetic strategies. *Coord. Chem. Rev.* **2013**, *257*, 1728−1763.

DOI: 10.1021/acs.inorgchem.7b02530
Inorg. Chem. XXXX, XXX, XXX−XXX

(5) Ishikawa, N.; Sugita, M.; Ishikawa, T.; Koshihara, S.; Kaizu, Y. Lanthanide Double-Decker Complexes Functioning as Magnets at the Single-Molecular Level. *J. Am. Chem. Soc.* **2003**, *125*, 8694−8695.
(6) Bechlars, B.; D'Alessandro, D. M.; Jenkins, D. M.; Iavarone, A. T.; Glover, S. D.; Kubiak, C. P.; Long, J. R. High-spin ground states via electron delocalization in mixed-valence imidazolate-bridged divanadium complexes. *Nat. Chem.* **2010**, *2*, 362−368.
(7) Jiang, S.-D.; Wang, B.-W.; Sun, H.-L.; Wang, Z.-M.; Gao, S. An Organometallic Single-Ion Magnet. *J. Am. Chem. Soc.* **2011**, *133*, 4730−4733.
(8) Wernsdorfer, W.; Rice, S. A.; Dinner, A. R. Classical and quantum magnetization reversal studied in nanometer sized particles and clusters. *Adv. Chem. Phys.* **2001**, *118*, 99−190.
(9) Bogani, L.; Wernsdorfer, W. Molecular spintronics using single-molecule magnets. *Nat. Mater.* **2008**, *7*, 179−186.
(10) Baker, M. L.; Blundell, S. J.; Domingo, N.; Hill, S. Spectroscopy Methods for Molecular Nanomagnets. *Struct. Bonding (Berlin, Ger.)* **2014**, *164*, 231−292.
(11) Nehrkorn, J.; Mukherjee, S.; Stuiber, S.; Mutka, H.; Strässle, Th.; Christou, G.; Waldmann, O. Ferromagnetic cluster spin waves in molecular disks studied by inelastic neutron scattering. *Phys. Rev. B: Condens. Matter Mater. Phys.* **2012**, *86*, 134417.
(12) Leuenberger, M. N.; Loss, D. Quantum computing in molecular magnets. *Nature* **2001**, *410*, 789−793.
(13) Oshio, H.; Hoshino, N.; Ito, T.; Nakano, M. Single-Molecule Magnets of Ferrous Cubes: Structurally Controlled Magnetic Anisotropy. *J. Am. Chem. Soc.* **2004**, *126*, 8805−8812.
(14) Yang, E.-C.; Hendrickson, D. N.; Wernsdorfer, W.; Nakano, M.; Zakharov, L. N.; Sommer, R. D.; Rheingold, A. L.; Ledezma-Gairaud, M.; Christou, G. Cobalt single-molecule magnet. *J. Appl. Phys.* **2002**, *91*, 7382−7384.
(15) Klinke, F. J.; Das, A.; Demeshko, S.; Dechert, S.; Meyer, F. Inducing Single Molecule Magnetic Behavior in a $[Co_4O_4]$ Cubane via a Pronounced Solvatomagnetic Effect. *Inorg. Chem.* **2014**, *53*, 2976−2982.
(16) Yang, E.-C.; Wernsdorfer, W.; Zakharov, L. N.; Karaki, Y.; Yamaguchi, A.; Isidro, R. M.; Lu, G.-D.; Wilson, S. A.; Rheingold, A. L.; Ishimoto, H.; Hendrickson, D. N. Fast Magnetization Tunneling in Tetranickel(II) Single-Molecule Magnets. *Inorg. Chem.* **2006**, *45*, 529−546.
(17) Gao, Y.; Xu, G.-F.; Zhao, L.; Tang, J. K.; Liu, Z. L. Observation of Slow Magnetic Relaxation in Discrete Dysprosium Cubane. *Inorg. Chem.* **2009**, *48*, 11495−11497.
(18) Ke, H. S.; Gamez, P.; Zhao, L.; Xu, G.-F.; Xue, S. F.; Tang, J. K. Magnetic Properties of Dysprosium Cubanes Dictated by the M-O-M Angles of the $[Dy_4(\mu_3\text{-}OH)_4]$ Core. *Inorg. Chem.* **2010**, *49*, 7549−7557.
(19) Gao, Y. J.; Zhao, L.; Xu, X. B.; Xu, G.-F.; Guo, Y.-N.; Tang, J. K.; Liu, Z. L. Heterometallic Cubanes: Syntheses, Structures, and Magnetic Properties of Lanthanide(III)-Nickel(II) Architectures. *Inorg. Chem.* **2011**, *50*, 1304−1308.
(20) Zhao, L.; Wu, J. F.; Ke, H. S.; Tang, J. K. Family of Defect-Dicubane Ni_4Ln_2 (Ln = Gd, Tb, Dy, Ho) and Ni_4Y_2 Complexes: Rare Tb(III) and Ho(III) Examples Showing SMM Behavior. *Inorg. Chem.* **2014**, *53*, 3519−3525.
(21) Ding, Y. S.; Chilton, N. F.; Winpenny, R. E. P.; Zheng, Y.-Z. On Approaching the Limit of Molecular Magnetic Anisotropy: A Near-Perfect Pentagonal Bipyramidal Dysprosium(III) Single-Molecule Magnet. *Angew. Chem., Int. Ed.* **2016**, *55*, 16071−16074.
(22) Murrie, M. Cobalt(II) single-molecule magnets. *Chem. Soc. Rev.* **2010**, *39*, 1986−1995.
(23) Kostakis, G. E.; Perlepes, S. P.; Blatov, V. A.; Proserpio, D. M.; Powell, A. K. High-nuclearity cobalt coordination clusters: Synthetic, topological and magnetic aspects. *Coord. Chem. Rev.* **2012**, *256*, 1246−1278.
(24) Zeng, M.-H.; Yao, M.-X.; Liang, H.; Zhang, W.-X.; Chen, X.-M. A Single-Molecule-Magnetic, Cubane-Based, Triangular Co_{12} Supercluster. *Angew. Chem., Int. Ed.* **2007**, *46*, 1832−1835.
(25) Zhou, Y.-L.; Zeng, M.-H.; Liu, X.-C.; Liang, H.; Kurmoo, M. Exploring the Effect of Metal Ions and Counteranions on the Structure and Magnetic Properties of Five Dodecanuclear Co^{II} and Ni^{II} Clusters. *Chem. - Eur. J.* **2011**, *17*, 14084−14093.
(26) Chen, Q.; Zeng, M.-H.; Zhou, Y.-L.; Zou, H.-H.; Kurmoo, M. Hydrogen-Bonded Dicubane Co^{II}_7 Single-Molecule-Magnet Coordinated by in Situ Solvothermally Generated 1,2-Bis(8-hydroxyquinolin-2-yl)-ethane-1,2-diol Arranged in a Trefoil. *Chem. Mater.* **2010**, *22*, 2114−2119.
(27) Zhou, Y.-L.; Zeng, M.-H.; Wei, L.-Q.; Li, B.-W.; Kurmoo, M. Traditional and Microwave-Assisted Solvothermal Synthesis and Surface Modification of Co_7 Brucite Disk Clusters and Their Magnetic Properties. *Chem. Mater.* **2010**, *22*, 4295−4303.
(28) Chen, Q.; Zeng, M.-H.; Wei, L.-Q.; Kurmoo, M. A Multifaceted Cage Cluster, $[Co^{II}_6O_{12} \supset X]^-$ (X = Cl^- or F^-): Halide Template Effect and Frustrated Magnetism. *Chem. Mater.* **2010**, *22*, 4328−4334.
(29) Zheng, Y.-Z.; Speldrich, M.; Schilder, H.; Chen, X.-M.; Kögerler, P. A tetranuclear cobalt(II) chain with slow magnetization relaxation. *Dalton Trans.* **2010**, *39*, 10827−10829.
(30) Fortier, S.; Le Roy, J. J.; Chen, C.-H.; Vieru, V.; Murugesu, M.; Chibotaru, L. F.; Mindiola, D. J.; Caulton, K. G. A Dinuclear Cobalt Complex Featuring Unprecedented Anodic and Cathodic Redox Switches for Single-Molecule Magnet Activity. *J. Am. Chem. Soc.* **2013**, *135*, 14670−14678.
(31) Zhang, Y.-Z.; Gao, S.; Sato, O. *In situ* tetrazole templated chair-like decanuclear azido-cobalt(II) SMM containing both tetra- and octahedral Co(II) ions. *Dalton Trans.* **2015**, *44*, 480−483.
(32) Nemec, I.; Herchel, R.; Machata, M.; Trávníček, Z. Tetranuclear Ni(II) and Co(II) Schiff-base complexes with an M_4O_6 defective dicubane-like core: zero-field SMM behavior in the cobalt analogue. *New J. Chem.* **2017**, *41*, 11258−11267.
(33) Wei, L.-Q.; Li, B.-W.; Hu, S.; Zeng, M.-H. Controlled assemblies of hepta- and trideca-Co^{II} clusters by a rational derivation of salicylalde schiff bases: microwave-assisted synthesis, crystal structures, ESI-MS solution analysis and magnetic properties. *CrystEngComm* **2011**, *13*, 510−516.
(34) Zhang, K.; Dai, J.; Wang, Y.-H.; Zeng, M.-H.; Kurmoo, M. Microwave and traditional solvothermal syntheses, crystal structures, mass spectrometry and magnetic properties of $Co^{II}_4O_4$ cubes. *Dalton Trans.* **2013**, *42*, 5439−5446.
(35) Nakano, M.; Oshio, H. Magnetic anisotropies in paramagnetic polynuclear metal complexes. *Chem. Soc. Rev.* **2011**, *40*, 3239−3248.
(36) Waldmann, O. Magnetic molecular wheels and grids - the need for novel concepts in "zero-dimensional" magnetism. *Coord. Chem. Rev.* **2005**, *249*, 2550−2566.
(37) Barszcz, B.; Jabłońska-Wawrzycka, A.; Stadnicka, K.; Jezierska, J. Coordination chemistry of 2-hydroxymethylbenzimidazole complexes with copper(II) and cadmium(II) ions: Similarities and differences. *Polyhedron* **2008**, *27*, 3500−3508.
(38) Zheng, L.-L.; Leng, J.-D.; Herchel, R.; Lan, Y.-H.; Powell, A. K.; Tong, M.-L. Anion-Dependent Facile Route to Magnetic Dinuclear and Dodecanuclear Cobalt Clusters. *Eur. J. Inorg. Chem.* **2010**, *2010*, 2229−2234.
(39) Zhang, M.; Yang, T.; Wang, Z.; Ma, X.-F.; Zhang, Y.; Greer, S. M.; Stoian, S. A.; Ouyang, Z.-W.; Nojiri, H.; Kurmoo, M.; Zeng, M.-H. Chemical reaction within a compact non-porous crystal containing molecular clusters without the loss of crystallinity. *Chem. Sci.* **2017**, *8*, 5356−5361.
(40) Zhang, S.-H.; Ma, L.-F.; Zou, H.-H.; Wang, Y.-G.; Liang, H.; Zeng, M.-H. Anion induced diversification from heptanuclear to tetranuclear clusters: Syntheses, structures and magnetic properties. *Dalton Trans.* **2011**, *40*, 11402−11409.
(41) Song, X.-Y.; Xu, Y.-H.; Li, L.-C.; Liao, D.-Z.; Jiang, Z.-H. An unexpected cubane-like nickel(II) tetranuclear complex bridged by the anion of 2-hydroxymethylbenzimidazole: Crystal structure and magnetic properties. *Inorg. Chim. Acta* **2007**, *360*, 2039−2044.
(42) Huang, L.; Zhong, A.-G.; Chen, D.-B.; Liang, H.-D. Synthesis, structure, spectroscopic properties, and theoretical studies of a new

DOI: 10.1021/acs.inorgchem.7b02530
Inorg. Chem. XXXX, XXX, XXX−XXX

blue/green luminescent complex: $[Cd_2Cl_4(Hbm)_2]_n \cdot nH_2O$ (Hbm = 1H-benzimidazol-2-ylmethanol). *J. Mol. Struct.* **2009**, *922*, 135−139.
(43) Goodenough, J. B. An interpretation of the magnetic properties of the perovskite-type mixed crystals $La_{1-x}Sr_xCoO_{3-\lambda}$. *J. Phys. Chem. Solids* **1958**, *6*, 287−297.
(44) Kanamori, J. Superexchange interaction and symmetry properties of electron orbitals. *J. Phys. Chem. Solids* **1959**, *10*, 87−98.
(45) Fabelo, O.; Pusan, J.; LLoret, F.; Julve, M.; Ruiz-Pérez, C. 1,2,4,5-Benzenetetracarboxylate- and 2,2′-Bipyrimidine-Containing Cobalt(II) Coordination Polymers: Preparation, Crystal Structure, and Magnetic Properties. *Inorg. Chem.* **2008**, *47*, 3568−3576.
(46) Kurmoo, M. Magnetic metal−organic frameworks. *Chem. Soc. Rev.* **2009**, *38*, 1353−1379.
(47) Chilton, N. F.; Anderson, R. P.; Turner, L. D.; Soncini, A.; Murray, K. S. PHI: A Powerful New Program for the Analysis of Anisotropic Monomeric and Exchange-Coupled Polynuclear *d*- and *f*-Block Complexes. *J. Comput. Chem.* **2013**, *34*, 1164−1175.
(48) Murrie, M.; Teat, S. J.; Stoeckli-Evans, H.; Güdel, H. U. Synthesis and Characterization of a Cobalt(II) Single-Molecule Magnet. *Angew. Chem., Int. Ed.* **2003**, *42*, 4653−4656.
(49) Galloway, K. W.; Whyte, A. M.; Wernsdorfer, W.; Sanchez-Benitez, J.; Kamenev, K. V.; Parkin, A.; Peacock, R. D.; Murrie, M. Cobalt(II) Citrate Cubane Single-Molecule Magnet. *Inorg. Chem.* **2008**, *47*, 7438−7442.
(50) Moubaraki, B.; Murray, K. S.; Hudson, T. A.; Robson, R. Tetranuclear and Octanuclear Cobalt(II) Citrate Cluster Single Molecule Magnets. *Eur. J. Inorg. Chem.* **2008**, *2008*, 4525−4529.
(51) Zhang, S.-H.; Zhang, Y. D.; Zou, H. H.; Guo, J. J.; Li, H. P.; Song, Y.; Liang, H. A family of cubane cobalt and nickel clusters: Syntheses, structures and magnetic properties. *Inorg. Chim. Acta* **2013**, *396*, 119−125.
(52) Guedes, G. P.; Soriano, S.; Comerlato, N. M.; Speziali, N. L.; Novak, M. A.; Vaz, M. G. F. Heptanuclear cobalt(II) dicubane compounds with single-molecule magnet behavior. *Inorg. Chem. Commun.* **2013**, *37*, 101−105.
(53) Roth, T.; Morningstar, M. L.; Boyer, P. L.; Hughes, S. H.; Buckheit, R. W., Jr.; Michejda, C. J. Synthesis and Biological Activity of Novel Nonnucleoside Inhibitors of HIV-1 Reverse Transcriptase. 2-Aryl-Substituted Benzimidazoles. *J. Med. Chem.* **1997**, *40*, 4199−4207.

DOI: 10.1021/acs.inorgchem.7b02530
Inorg. Chem. XXXX, XXX, XXX−XXX